Acetaminophen production in the edible, filamentous cyanobacterium *Arthrospira platensis*

Jacob M. Hilzinger[1], Skyler Freidline[1], Divya Sivanandan[1], Ya-Fang Cheng[2], Shunsuke Yamazaki[1,3], Douglas S. Clark[4,5], Jeffrey M. Skerker[1], Adam P. Arkin[1,6,*]

Author Affiliations:

1-Department of Biological Engineering, University of California-Berkeley, Berkeley, CA 94720, USA

2-QB3-Berkeley, University of California, Berkeley, CA 94720, USA

3-Ajinomoto Co., Inc., 1-1 Suzuki-cho, Kawasaki, Kanagawa 210-8681, Japan

4-Department of Chemical and Biomolecular Engineering, University of California-Berkeley, Berkeley, CA 94720, USA

5-Molecular Biophysics and Integrated Bioimaging Division, Lawrence Berkeley National Laboratory, 1 Cyclotron Road, Berkeley, CA 94720, USA

6-Environmental Genomics and Systems Biology Division, Lawrence Berkeley National Laboratory, 1 Cyclotron Road, Berkeley, CA 94720, USA

*- Correspondence should be addressed to A.P.A. (aparkin@lbl.gov)

Keywords: Cyanobacteria, Spirulina, *Arthrospira platensis*

Abstract

Spirulina is the common name for the edible, non-heterocystous, filamentous cyanobacterium *Arthrospira platensis* that is grown industrially as a food supplement, animal feedstock, and pigment source. Although there are many applications for engineering this organism[1–3], until recently no genetic tools or reproducible transformation methods have been published. While recent work showed the production of single domain antibodies for oral delivery, no publicly available genetic toolkit was provided[4]. Here, we establish a genetic toolkit and reproducible method for the transformation of *A. platensis* and engineer this bacterium to produce acetaminophen as proof-of-concept for small molecule production in an edible host from CO_2, H_2O, and light. This work opens *A. platensis* to the wider scientific community for future engineering as a functional food for nutritional enhancement, modification of organoleptic traits, and production of pharmaceuticals for oral delivery.

Introduction

Arthrospira platensis, commonly referred to and sold commercially as spirulina, is an edible, non-heterocystous, filamentous cyanobacterium of the order *Oscillatoriales*, with species of this genus having been used as traditional food sources in Mexico and Chad for centuries[5,6]. *A. platensis* is considered safe for human consumption and is designated as Generally Recognized as Safe (GRAS) by the U.S. Food and Drug Administration (GFA GRN No. 417); it has exceptionally high protein content relative to plants and eukaryotic microalgae[1], and is grown commercially as a food, pigment source, and animal feedstock[1,6]. Given its enticing food properties and established commercial growth, as well as applications driven by a photosynthetic metabolism, there is keen interest in genetically modifying this bacterium for enhanced nutrition, modified organoleptic traits, improved growth properties, and pharmaceutical production[1,2,4].

While there are clear applications for sustainable biomanufacturing on Earth, the edible nature and photosynthetic metabolism of *A. platensis* makes it well-suited as an alternate food source and microbial host for on-demand pharmaceutical production for *in situ* resource utilization (ISRU)-based missions for human space exploration and habitation[7–9]. As humans delve deeper into space via the Moon and eventually to Mars and beyond, the need to reduce mission launch cost, reduce risk, and anticipate pharmaceutical degradation induced by radiation becomes paramount, further increasing the need for ISRU-driven food and pharmaceutical

51 production[3,7,10–13]. NASA and ESA have both established the utility of this organism for space
52 exploration via their biological life support projects, CELSS and MELISSA, respectively, which
53 used *A. platensis* to photoautotrophically recycle NO_3^- and CO_2 for production of O_2 and
54 biomass for astronaut consumption[14,15]. Expanding upon its established life support properties to
55 further produce functional foods for nutrition and pharmaceutical delivery will further increase
56 the utility of this organism for deep space missions.
57 *A. platensis* has historically remained recalcitrant to the development of genetic tools and
58 a reproducible transformation method[16–19]. Potential reasons range from its multicellularity,
59 polyploidy, and motility, which combine to inhibit colony formation on plates, and a genome
60 that encodes a high number of restriction modification systems of types I-IV in addition to
61 several CRISPR/Cas systems[20,21]. However, in a landmark study, Jester *et al.* (2022) recently
62 engineered *A. platensis* for antibody production targeting campylobacter infections, and showed
63 that their orally-delivered strain prevents disease in mice and is safe for human consumption[4].
64 While this work provided a transformation method, a robust, publicly available genetic toolkit
65 for pathway engineering of *A. platensis* remains unavailable. This limitation, combined with the
66 general difficulty of performing genetic manipulations in this bacterium, have so far prevented *A.*
67 *platensis* from being engineered for small molecule production.
68 Here, we develop two reproducible transformation methods based on electroporation and
69 natural competence, use these methods to develop and characterize a genetic toolkit for
70 downstream pathway engineering, and engineer *A. platensis* to produce acetaminophen as proof-
71 of-concept for small molecule production derived from CO_2, H_2O, and light in an edible host for
72 bioavailable, oral drug delivery.
73
74 **Results**
75 We initially developed an electroporation method inspired by the patent literature[22] (see
76 Methods for details). Due to its filamentous and motile nature, *A. platensis* does not form
77 colonies on plates, and we were unable to obtain filament or cell counts. Thus, we were unable to
78 quantify plating or transformation efficiency, and were therefore dependent on the binary output
79 of growth or no growth, as has been observed in *Phormidium lacuna*[23]. Based on the predictions
80 of Nies *et al.* (2020), we confirmed natural competence in *A. platensis*, and established this
81 method as our standard transformation procedure.

82 Cyanobacteria have a wide range of genome copy numbers per cell[24], with reported copy
83 numbers of the *Oscillatoriales* ranging from 20-90 copies per cell in *Phormidium lacuna*[23] to
84 nearly 700 in *Trichodesmium erythreaum* IMS 101[25]. For all transformations resulting in
85 biomass under selection, we observed that transformant biomass encoded the native locus in
86 addition to the exogenous DNA (data not shown), suggesting an initial integration into the
87 genome without full segregation through the genome and/or filament. Transformant biomass was
88 subcultured until no native locus could be detected via PCR and/or genome sequencing. This
89 took approximately 3-4 months on agar plates and 2-3 months in liquid culture (data not shown).
90 Jester *et al.* (2022) reported a segregation time of 8-10 weeks for *A. platensis*[4], further supporting
91 our observations that exogenous DNA must be selected over long timeframes through a
92 polyploid genome and multi-cell filament.
93 We established a series of working parts in *A. platensis* NIES-39: one antibiotic
94 resistance marker, three genomic loci for insertion of exogenous DNA, four endogenous and five
95 exogenous promoters, and one fluorescent reporter (Supplemental Table 1). All parts were
96 integrated into a series of suicide vectors for homologous recombination with the genome
97 (Supplemental Table 2). To screen multiple loci as genomic integration sites, we chose neutral
98 site I (NSI; NIES39_Q01230), a commonly used site in other cyanobacteria for insertion of
99 exogenous DNA[26], along with two loci we expected to be involved in motility to potentially
100 create non-motile strains to aid in plating and genetics.
101 Twitching motility in cyanobacteria is dependent on Type IV pili and is light regulated
102 resulting in phototaxis towards or away from light sources[27,28]. Filamentous cyanobacteria from
103 the *Oscillatoriales* and certain species of the *Nostocales* employ surface-dependent gliding
104 motility, with the oscillin protein from *Phormidium uncinatum* being essential for this type of
105 motility[27,29]. We targeted *pilA* (NIES39_C03030), a central component of the Type-IV pilin
106 system, and an oscillin homolog (NIES39_A01430) as integration sites for exogenous DNA and
107 motility ablation. We knocked out these three loci with the codon optimized version of *aadA*,
108 *aadA.co*, which encodes for streptomycin/spectinomycin (Sm/Sp) resistance (Fig. 1;
109 Supplemental Table 2). The ΔNSI::P*pilA-aadA.co*, Δoscillin::*aadA.co*, and Δ*pilA*::*aadA.co*
110 strains were confirmed by whole genome sequencing (Fig. 1A). Of note, Δ*pilA*::*aadA.co* mutants
111 display a "star" morphology when plated on agar, while Δoscillin::*aadA.co* mutants display a

112 “string” morphology (Fig. 1). This implies that both genes are involved in motility and/or colony
113 formation on plates.
114 Deletion of the NSI locus does not result in morphological or growth differences between
115 the wild type (WT) strain as expected (Fig. 1). Light-based motility assays showed that the WT
116 and ΔNSI::P*pilA-aadA.co* strains moved into the illuminated area of the plate within seven days,
117 while the Δoscillin::*aadA.co* and Δ*pilA*::*aadA.co* strains remained in the shade where they were
118 initially spotted (Fig. 1C). While the Δ*pilA*::*aadA.co* strain did not expand beyond its initial spot,
119 the Δoscillin::*aadA.co* mutant moved in a small halo around the initial spot, indicating that
120 motility is severely limited by, but not entirely dependent on, the loss of oscillin. This indicates
121 that both *pilA* and oscillin genes contribute to phototaxis in *A. platensis*.
122 To test an expression system in *A. platensis*, we designed a series of vectors
123 (Supplemental Table 2) that resulted in mutant strains at the *pilA* locus that had one of three
124 native, strong promoters (P_{psaA}, P_{cpcB}, or P_{rbcL})[30] or one of five J23-series promoters driving the
125 expression of codon optimized *eYFP* (*eYFP.co*) downstream of the native *pilA* promoter driving
126 the expression of *aadA.co* followed by the native *aadA* terminator (Fig. 2A). The fluorescent
127 output of each strain was measured, showing orders of magnitude higher fluorescence in the
128 eight reporter strains than in the WT (Fig. 2B). The J23-series promoters displayed a 4-fold
129 dynamic range in *A. platensis* compared to a 120-fold dynamic range in both *Synechococcus*
130 *elongatus* UTEX 2973 and *Synechocystis* sp. 6803[31]. Although methodological differences
131 between these studies may explain some of this difference, these results highlight the need for
132 further development and characterization of *A. platensis* specific genetic parts. Fluorescence was
133 manually checked under a fluorescence microscope to confirm expression of eYFP.co in the
134 reporter strains; no fluorescence was detected in the WT strain (Fig. 2C).
135 For the biosynthesis of acetaminophen (APAP; Fig. 3A), chorismate is converted into
136 para-aminobenzoic acid (PABA) by the multienzyme complex PabABC, composed of
137 aminodeoxychorismate synthase (pabAB) and 4-amino-4-deoxychorismate lyase (pabC). PABA
138 is converted into 4-aminophenol by the 4-aminobenzoate hydrolase (4ABH) from *Agaricus*
139 *bisporus*, which is subsequently converted to APAP by N-hydroxyarylamine O-acetyltransferase
140 (NhoA) from *Escherichia coli*[32]. A series of 38 suicide vectors encoding variations on the
141 synthetic APAP biosynthesis pathway with codon optimized genes (Fig. 3A) were designed and
142 screened in *A. platensis* (Supplemental Table 3). Of these, 23 resulted in transformant biomass

143 that displayed the WT morphology under selection at 1 µg/ml Sm/Sp; no transformants for any
144 vector could be recovered at higher selection strengths.
145 For every transformation, a negative control was run to ensure that the selection killed
146 WT cells, and pJMH024 was transformed as a positive control to ensure that cells were
147 transformable. PCR screens of genomic DNA isolated from transformant biomass indicated the
148 presence of *pilA*, *aadA.co*, *4ABH*, and *nhoA* (data not shown), suggesting an initial integration of
149 the suicide vector into the genome. However, no transformant biomass resulting from any of
150 these vectors grew after subculturing into the same growth conditions. The only way we could
151 recover a fully segregated strain, APA16206 (Fig. 3B), was under 16h light:8h dark cycles
152 illuminated with ~20-30 µmol m^{-2} s^{-1} (µEi) of photosynthetically active radiation (see Methods
153 for details) for three months until star morphology appeared. Tufts of star morphology were
154 subcultured into fresh selective medium under the same conditions. Upon reaching mid to late
155 log phase, biomass was subcultured and grown under 24h light illuminated with ~70-100 µEi.
156 Biomass was regularly subcultured under these conditions upon reaching mid to late log phase
157 until fully segregated (Supplemental Fig. 1).
158 As PABA supplementation was previously shown to increase APAP titer[32], we screened
159 APAP production in the WT and APA16206 strains with and without the addition of the
160 precursor compound, PABA (Fig. 3C-E; Supplemental Fig. 2). The WT strain did not produce
161 APAP under any condition, while the mutant produced APAP only when PABA was added to
162 the medium (Fig. 3C). The APAP titer and production rate in APA16206 were dependent on the
163 amount of PABA supplied, with titer and rate increasing with increasing PABA concentrations.
164 The maximal titer and rate were 2.9 mg L^{-1} and 0.018 mg L^{-1} hr^{-1}, respectively, when supplied
165 with 2.74 g L^{-1} PABA. Growth rate was slowed by increasing PABA concentration, but did not
166 impact the final biomass yield, except for two of the replicates supplemented with 2.74 g L^{-1}
167 PABA, which prematurely reached stationary phase and died (Fig. 3E). The APAP production
168 rate appeared dependent on the growth rate.
169
170 **Discussion**
171 Here we independently establish the reproducible transformation of *A. platensis* via
172 electroporation and natural competence, characterize an initial genetic toolkit for pathway
173 engineering, and produce APAP as a proof-of-concept pharmaceutical for oral delivery. Our

174 methods help unlock this bacterium for future engineering efforts for sustainable
175 biomanufacturing on Earth and ISRU-based food and pharmaceutical production in space by
176 providing a reproducible blueprint. Building on recent work[4,23], we help establish genetic
177 tractability in the *Oscillatoriales,* an order of cyanobacteria that have been historically
178 understudied through genetic methods. Members of this order, such as the diazotrophic genus
179 *Trichodesmium*, are major contributors to the biological nitrogen cycle.
180 While our open-source genetic toolkit and proof-of-concept biosynthesis of APAP is an
181 important step for metabolically engineering *A. platensis*, continued improvement in the genetic
182 tools available is paramount to decrease the design-build-test-learn cycle time in this bacterium.
183 Crucial to this endeavor is the development of new promoters to overcome the limited dynamic
184 range we observed, which may be achieved through the characterization of alternate native
185 promoters, synthetic promoters engineered from native promoters, or the establishment of
186 inducible promoters[33]. Operationalizing a CRISPR/Cas system[34] would provide a locus-
187 independent counterselection that may decrease the segregation time, as the Cas enzyme would
188 be expected to cut all, or most, genome copies present in the cell, , and would allow for
189 installation of more complex pathways. Developing self-replicating vectors for the expression of
190 pathways or a CRISPR/Cas system would bypass the need for genome integration, and allow for
191 rapid screening of pathway topologies and simpler CRISPR/Cas-based genome engineering.
192 APAP is the first reported exogenous small molecule produced in *A. platensis* and
193 provides a milestone in the long-term efforts to genetically engineer this organism. Given that a
194 dose of APAP is 325 mg, our maximum titer of 2.9 mg/L would require ~112 L for a single dose,
195 assuming complete bioavailability. Thus, higher titer will need to be achieved to make
196 manufacturing a dose of APAP feasible if oral delivery via spirulina is the goal. To this end,
197 there are several routes that should be explored.
198 Of the 38 APAP pathway topologies we transformed into *A. platensis*, we could only
199 recover one fully segregated mutant that, in turn, could only be recovered under day/night cycles.
200 This was in stark contrast to the creation of other mutants reported here, which proceeded
201 without difficulty, and suggests that enzyme toxicity from 4ABH and/or NhoA, due to their
202 products or the enzymes themselves, inhibited integration and/or segregation of the pathway into
203 and through the genome. Several additional, unknown chromatography peaks were observed in
204 APA16206 when PABA was supplied (Fig. 3C), and may contribute to the observed pathway

205 toxicity. These unknown peaks eluted at similar times as PABA and APAP, implying a similar
206 chemical structure. These peaks may be due to enzyme promiscuity of 4ABH and/or NhoA, or
207 from APAP degradation products; these peaks are not from the intermediate 4-aminophenol as
208 the standard for this molecule produced two peaks at elution times of 2.9 and 3.3 min (data not
209 shown). If these compounds are produced from enzyme promiscuity, engineering a strain to
210 produce only APAP would likely increase the titer of APAP by avoiding flux of PABA into
211 these accessory compounds. This could be done through enzyme engineering, removing
212 biosynthesis pathways from the genome for substrates that these enzymes may promiscuously
213 convert, or screening 4ABH and/or NhoA homologs for improved selectivity towards APAP
214 production. Decreasing the potential pathway toxicity through use of weaker promoters, enzyme
215 scaffolding, or enzyme engineering for higher product selectivity may make this pathway more
216 engineerable for future iterations towards a higher titer.
217 PABA was not detected in either strain without PABA supplementation. This may be due
218 to natively low flux through PABA or a high rate of PABA turnover. However, while we were
219 able to identify a homolog for PabAB (NIES39_E04160), we were unable to identify a homolog
220 for characterized PabC proteins[35–37] in the *A. platensis* genome. While there may be an
221 uncharacterized PabC, there is a chance that PABA is not natively produced by *A. platensis*,
222 which would be unexpected as PABA is a precursor for folate. Establishing and/or increasing
223 endogenous PABA biosynthesis could increase APAP titer, or, crucially, allow for production
224 without PABA supplementation. As the APAP yield from supplied PABA was ~0.1%, a
225 sufficient intracellular production rate of PABA may be easily achievable to reach APAP
226 production rates observed with supplementation. This may also alleviate the observed toxicity
227 from PABA when supplied at high extracellular concentrations (Fig. 3D). Engineering *A.*
228 *platensis* for sufficient PABA production would also remove the economic burden of PABA
229 supplementation for scale-up.
230 The genetic toolkit and methods we provide here pave the way for the diversification of
231 commodity chemicals and biologics to be produced in *A. platensis* beyond APAP and single
232 domain antibodies[4]. Decisions on which molecules to produce would benefit from a combination
233 of technoeconomic and life cycle analyses targeting high value products such as pharmaceuticals
234 and cannabinoids. This work further opens *A. platensis* as an engineerable, functional food.
235 Modification of organoleptic traits and nutritional properties may lead to more palatable and

236 nutritious strains for improved consumption by humans or for animal feedstocks. Improved
237 genetic tools along with host optimization; for example, through the removal of restriction
238 modification systems, genome copy number control, and morphological control, may further
239 improve the engineerability of this organism. The present work is thus an important step towards
240 realizing the potential of an industrially grown, edible, photosynthetic organism for the oral
241 delivery of pharmaceuticals and nutritional compounds.
242
243 **Methods**
244 **Growth and transformation of *Arthrospira platensis*.** A list of strains used in this study can be
245 found in Supplemental Table 2. WT *A. platensis* NIES-39, obtained from the NIES culture
246 collection, was grown in Zarrouk's Medium (ZM)[38] at 30°C under ~70-100 µmol photons m^{-2} s^{-1}
247 (µEi) of photosynthetically active radiation produced by cool, white LEDs (compact LED bars
248 from Photon Systems Instruments controlled by their LC 200 light controller) with shaking at
249 200 rpm unless stated otherwise. Working streptomycin/spectinomycin (Sm/Sp) concentrations
250 ranged from 1-100 µg/ml.
251 For electroporations, WT *A. platensis* NIES-39 cells were grown to early log phase
252 (OD_{750} ~0.2-0.3), washed three times with room temperature, sterile water and concentrated to
253 150 µg Chl *a* ml^{-1} in sterile water. Chl *a* concentration was measured based on the methods of
254 Meeks and Castenholz (1971)[39]. For each electroporation reaction, 400 µl concentrated cells
255 were mixed with 10 µg plasmid on ice, transferred to a cold 2 mm electroporation cuvette, and
256 electroporated at 600 V with a time constant of ~6-7 ms^{-1} on a BTX Gemini electroporator. Cells
257 were recovered in a final volume of 1 ml ZM, and grown overnight (~15-20 hours) at 30°C under
258 ~20-30 µEi with shaking. The following day, cells were washed once with ZM + Sm/Sp[1], and
259 plated onto selective 1.5% Bacto agar (BD #214010) plates or into selective liquid ZM in
260 multiwell (96-, 24-, 12-, and/or 6-well) plates. Biomass was selectively passaged onto plates and
261 into liquid media, and monitored via PCR and/or Illumina sequencing until fully segregated.
262 For natural transformations, WT *A. platensis* NIES-39 cells were grown to early log
263 phase (OD_{750} ~0.2-0.3) and concentrated to 150 µg Chl *a* ml^{-1} in ZM. 100 µl concentrated cells
264 were mixed with 2.5 µg plasmid DNA, and incubated for 45 min at room temperature. Cells
265 were recovered in a final volume of 1 ml ZM, and grown overnight (~15-20 hours) at 30°C under
266 ~20-30 µEi with shaking. Recovered cells were added to 99 ml ZM + Sm/Sp (1-10 µg/ml) in

267 250-ml flasks, and incubated under ~20-30 µEi until growth appeared. Biomass was subcultured
268 under increasing concentrations of Sm/Sp (up to 100 µg/ml) until fully segregated as monitored
269 by PCR.
270
271 **Genomic DNA Extraction**. gDNA was extracted as follows: 1-ml aliquots of culture were
272 harvested by centrifugation. Pelleted cells were resuspended in 300 µl ELB (20 mM Tris-HCl, 2
273 mM Na-EDTA, 1.2% Triton-X). Cell suspension was incubated at room temperature for 30 min
274 with 2,500 units of Ready-Lyse lysozyme (Lucigen #R1804M) and 200 µg RNase A (Qiagen
275 #19101). An additional 2,500 units of lysozyme were added and incubated for 30 min at room
276 temperature. 15 µl of Proteinase K (20 mg/ml; Qiagen #19157) were added to the suspension and
277 incubated at 65°C for approximately one hour. 400 µl phenol:chloroform:isoamyl alcohol
278 (25:24:1 v/v; Sigma #P3803) were mixed with the cell suspension, and centrifuged for 5 min at
279 21,130 *x* g. 30 µl of 3M sodium acetate + 0.1M EDTA were added to the aqueous phase,
280 followed by 660 µL cold 100% ethanol, and centrifuged for 15 min at 21,130 *x* g. Supernatant
281 was removed, and the pellet was washed once with 1 mL 70% EtOH. Following removal of the
282 wash, the pellet was air dried for 5 minutes prior to resuspension in nuclease-free TE buffer
283 (Thermo Scientific #J75793).
284
285 **Next Generation Sequencing.** Library preparation and 250 bp paired-end sequencing on an
286 Illumina HiSeq 4000 was completed by the QB3 Genomics, UC Berkeley, Berkeley, CA,
287 RRID:SCR_022170.
288
289 **Data analysis.** Raw Illumina NovaSeq sequencing reads were processed as follows. Burrows-
290 Wheeler Alignment tool (BWA)[40] was used to index the reference genome AP011615, align
291 sequencing reads and generate a sam file. Samtools[41] was used to convert the data to a bam file
292 and then sort and index the alignments. Picard's DownsampleSam
293 (https://broadinstitute.github.io/picard/) was used to downsample the BAM files to ~10% of the
294 total depth for visualization in Geneious. Geneious was used to visualize the alignments and
295 generate figures.
296

297 **Motility assays.** ZM solidified with 0.5% agar was poured into each lane of a 4-well plate.
298 Cultures of each strain to be assayed were inoculated to a starting OD_{750} of 0.05 and allowed to
299 grow until mid-log phase (OD_{750} = 0.5 – 0.7). A volume of each culture equal to 750 µL OD_{750} =
300 1.0 was pelleted by centrifugation and the supernatant was removed. The cell pellets were
301 collected and dispensed at one end of an agar lane in the 4-well plate. The plate was sealed and
302 imaged immediately. The plate was moved to a 30°C room and placed directly under cool, white
303 LEDs at a flux of 50 µEi. The half of the plate containing the cell pellets was placed in a
304 protective covering to prevent direct exposure to light and encourage growth to the far end of the
305 plate. The plate was imaged every 24 hours for 7 days.
306
307 **Vector design and synthesis.** A list of vectors can be found in Supplemental Table 2. All genes
308 were codon optimized, purged of the restriction modification (RM) sites (see below),
309 synthesized, and cloned by Genscript Corp. The remaining parts were synthesized and cloned by
310 Genscript Corp. The purged RM sites can be found in Supplemental Table 4. This list was
311 compiled from literature and homology searches[20,42,43].
312
313 **Fluorescence microscopy.** Mid-log phase cultures were imaged on a Zeiss Observer D1
314 fluorescence microscope. Chlorophyll autofluorescence was imaged under excitation at 587 nm
315 and emission at 610 nm and eYFP fluorescence was measured under excitation at 495 nm and
316 emission at 527 nm. Images were falsely colored using Zeiss Zen Pro version 3.5.
317
318 **Quantification of promoter strengths.** *A. platensis* WT and mutant strains were each grown in
319 eight wells of triplicate 96-well plates under ~20-30 µEi without shaking at 30°C. OD_{750} and
320 eYFP fluorescence (excitation at 485 nm and emission at 535 nm) were measured daily on a
321 Tecan Spark M10 plate reader, and these values were normalized to blank measurements.
322
323 **HPLC.** Acetaminophen (APAP) and para-aminobenzoic acid (PABA) were quantified on a
324 Shimadzu Prominence HPLC system equipped with a photodiode array detector for UV
325 detection. Compounds were separated on a Zorbax StableBond Plus C18 5 µm with detection at
326 240 nm. The elution protocol was based on a gradient method using (A) 0.1% phosphoric acid

327 and (B) methanol as follows: 0 min - 95% A, 5% B; 15 min 100% B; 16-20 min 95% A, 5% B at
328 a flow rate of 1 ml min^{-1}.
329 For sample preparation, 1 ml culture was transferred to a BeadBug bead beating tube
330 (Millipore Sigma #Z763748) and vortexed on high for 10 minutes. Samples were then
331 centrifuged for 10 min at 14k rpm. 800 µl supernatant were filtered through 13 mm 0.2 µm
332 PVDF syringe filters (Pall #4406). Standards were prepared in volumetric flasks using APAP
333 (Sigma #A5000) and PABA (Sigma #A9878), and serially diluted in ZM. The 4-aminophenol
334 (Sigma #A71328) standard was prepared similarly using methanol as the solvent.
335

336 **Acknowledgements**
337 This work was supported by the Center for the Utilization of Biological Engineering in Space
338 (CUBES, https://cubes.space), a NASA Space Technology Research Institute (grant number
339 NNX17AJ31G) and by NIH S10 OD018174 Instrumentation Grant. We thank Kyle Sander,
340 Aaron Berliner, Kelly Wetmore, Kelsey Hern, and Yolanda Huang for useful discussions and
341 support.
342

343 **Author Contributions**
344 J.M.H., J.M.S., and A.P.A. conceived the project. J.M.H., S.F., J.M.S., and A.P.A. designed
345 experimental work. J.M.H., S.F., D.S., S.Y., and J.M.S. performed experimental work. J.M.H.,
346 S.F., J.M.S., and A.P.A. analyzed data. Y.C. developed the HPLC method. J.M.H., S.F., J.M.S.,
347 D.S.C., and A.P.A wrote the manuscript.
348

349 **Supplementary Data**
350 Plasmid maps for plasmids listed in Supplementary Tables 2 and 3 are available at
351 https://doi.org/10.6084/m9.figshare.20085284.
352

353 **References**
354 1. Torres-Tiji, Y., Fields, F. J. & Mayfield, S. P. Microalgae as a future food source.
355 *Biotechnol. Adv.* **41**, 107536 (2020).
356 2. Furmaniak, M. A. *et al.* Edible cyanobacterial genus *Arthrospira*: Actual state of the art in
357 cultivation methods, genetics, and application in medicine. *Front. Microbiol.* **8**, 1–21

358 (2017).
359 3. Berliner, A. J. *et al.* Towards a Biomanufactory on Mars. **8**, 1–20 (2020).
360 4. Jester, B. W. *et al.* Development of spirulina for the manufacture and oral delivery of
361 protein therapeutics. *Nat. Biotechnol.* **40**, 1-9 (2022).
362 5. Ciferri, O. Spirulina, the Edible Microorganism. *Microbiol. Rev.* **47**, 551–578 (1983).
363 6. Vonshak, A. *Spirulina plantesis (Arthrospira): Physiology, Cell-biology and*
364 *Biotechnology*. (2002).
365 7. Nangle, S. N. *et al.* The case for biotech on Mars. *Nature Biotechnology* **38**, 401–407
366 (2020).
367 8. McNulty, M. J. *et al.* Molecular pharming to support human life on the moon, mars, and
368 beyond. *Crit. Rev. Biotechnol.* **41**, 849–864 (2021).
369 9. Mapstone, L. J., Leite, M. N., Purton, S., Crawford, I. A. & Dartnell, L. Cyanobacteria
370 and microalgae in supporting human habitation on Mars. *Biotechnol. Adv.* **59**, 107946
371 (2022).
372 10. Menezes, A. A., Montague, M. G., Cumbers, J., Hogan, J. A. & Arkin, A. P. Grand
373 challenges in space synthetic biology. *J. R. Soc. Interface* **12**, 20150803 (2015).
374 11. Menezes, A. A., Cumbers, J., Hogan, J. A. & Arkin, A. P. Towards synthetic biological
375 approaches to resource utilization on space missions. *J. R. Soc. Interface* **12**, 20140715
376 (2015).
377 12. Blue, R. S. *et al.* Supplying a pharmacy for NASA exploration spaceflight: challenges and
378 current understanding. *npj Microgravity* **5**, 14 (2019).
379 13. Blue, R. S. *et al.* Limitations in predicting radiation-induced pharmaceutical instability
380 during long-duration spaceflight. *npj Microgravity* **5**, 15 (2019).
381 14. Tadros, M. G. Characterization of Spirulina Biomass for CELSS Diet Potential. *NASA*
382 *Contract.* **2–501**, 53 (1988).
383 15. Gòdia, F. *et al.* MELISSA: A loop of interconnected bioreactors to develop life support in
384 Space. *J. Biotechnol.* **99**, 319–330 (2002).
385 16. Toyomizu, M., Suzuki, K., Kawata, Y., Kojima, H. & Akiba, Y. Effective transformation
386 of the cyanobacterium Spirulina platensis using electroporation. *J. Appl. Phycol.* **13**, 209–
387 214 (2001).
388 17. Kawata, Y., Yano, S., Kojima, H. & Toyomizu, M. Transformation of Spirulina platensis

389 strain C1 (Arthrospira sp. PCC9438) with Tn5 transposase-transposon DNA-cation
390 liposome complex. *Mar. Biotechnol.* **6**, 355–363 (2004).
391 18. Jeamton, W., Dulsawat, S., Tanticharoen, M., Vonshak, A. & Cheevadhanarak, S.
392 Overcoming intrinsic restriction enzyme barriers enhances transformation efficiency in
393 *Arthrospira platensis* C1. *Plant Cell Physiol.* **58**, 822–830 (2017).
394 19. Dehghani, J. *et al.* Stable transformation of *Spirulina* (*Arthrospira*) *platensis*: a promising
395 microalga for production of edible vaccines. *Appl. Microbiol. Biotechnol.* **102**, 9267–9278
396 (2018).
397 20. Fujisawa, T. *et al.* Genomic structure of an economically important cyanobacterium,
398 *Arthrospira* (*Spirulina*) *platensis* NIES-39. *DNA Res.* **17**, 85–103 (2010).
399 21. Silas, S. *et al.* On the origin of reverse transcriptase- using CRISPR-Cas systems and their
400 hyperdiverse, enigmatic spacer repertoires. *MBio* **8**, e00897-17 (2017).
401 22. Takeuchi, R. & Roberts, J. Targeted Mutagenesis in Spirulina. (2017).
402 23. Nies, F., Mielke, M., Pochert, J. & Lamparter, T. Natural transformation of the
403 filamentous cyanobacterium *Phormidium lacuna*. *PLoS One* **15**, 1–18 (2020).
404 24. Griese, M., Lange, C. & Soppa, J. Ploidy in cyanobacteria. *FEMS Microbiol. Lett.* **323**,
405 124–131 (2011).
406 25. Sargent, E. C. *et al.* Evidence for polyploidy in the globally important diazotroph
407 *Trichodesmium*. *FEMS Microbiol. Lett.* **363**, 1–7 (2016).
408 26. Taton, A. *et al.* Broad-host-range vector system for synthetic biology and biotechnology
409 in cyanobacteria. *Nucleic Acids Res.* **42**, e136 (2014).
410 27. Brahamsha, B. & Bhaya, D. Motility in Unicellular and Filamentous Cyanobacteria. *The*
411 *Cell Biology of Cyanobacteria* 233–262 (2013).
412 28. Schuergers, N., Mullineaux, C. W. & Wilde, A. Cyanobacteria in motion. *Curr. Opin.*
413 *Plant Biol.* **37**, 109–115 (2017).
414 29. Hoiczyk, E. & Baumeister, W. Oscillin, an extracellular, Ca2+-binding glycoprotein
415 essential for the gliding motility of cyanobacteria. *Mol. Microbiol.* **26**, 699–708 (1997).
416 30. Wang, B., Wang, J. & Meldrum, D. R. Application of synthetic biology in cyanobacteria
417 and algae. *Front. Microbiol.* **3**, 1–15 (2012).
418 31. Vasudevan, R. *et al.* Cyanogate: A modular cloning suite for engineering cyanobacteria
419 based on the plant moclo syntax. *Plant Physiol.* **180**, 39–55 (2019).

420 32. Anderson, J. C. Biosynthetic production of acetaminophen, p-aminophenol, and p-
421 aminobenzoic acid. (2017).
422 33. Behle, A., Saake, P., Germann, A. T., Dienst, D. & Axmann, I. M. Comparative Dose-
423 Response Analysis of Inducible Promoters in Cyanobacteria. *ACS Synth. Biol.* **9**, 843–855
424 (2020).
425 34. Ungerer, J. & Pakrasi, H. B. Cpf1 Is A Versatile Tool for CRISPR Genome Editing
426 Across Diverse Species of Cyanobacteria. *Sci. Rep.* **6**, 1–9 (2016).
427 35. Green, J. M., Merkel, W. K. & Nichols, B. P. Characterization and sequence of
428 Escherichia coli *pabC*, the gene encoding aminodeoxychorismate lyase, a pyridoxal
429 phosphate-containing enzyme. *J. Bacteriol.* **174**, 5317–5323 (1992).
430 36. Satoh, Y., Kuratsu, M., Kobayashi, D. & Dairi, T. New gene responsible for para-
431 aminobenzoate biosynthesis. *J. Biosci. Bioeng.* **117**, 178–183 (2014).
432 37. de Crécy-Lagard, V., El Yacoubi, B., de la Garza, R. D., Noiriel, A. & Hanson, A. D.
433 Comparative genomics of bacterial and plant folate synthesis and salvage: Predictions and
434 validations. *BMC Genomics* **8**, 1–15 (2007).
435 38. Madkour, F. F., Kamil, A. E. W. & Nasr, H. S. Production and nutritive value of Spirulina
436 platensis in reduced cost media. *Egypt. J. Aquat. Res.* **38**, 51–57 (2012).
437 39. Meeks, J. C. & Castenholz, R. W. Growth and photosynthesis in an extreme thermophile,
438 *Synechococcus lividus* (*Cyanophyta*). *Arch. Mikrobiol.* **78**, 25–41 (1971).
439 40. Li, H. & Durbin, R. Fast and accurate short read alignment with Burrows-Wheeler
440 transform. *Bioinformatics* **25**, 1754–1760 (2009).
441 41. Danecek, P. *et al.* Twelve years of SAMtools and BCFtools. *Gigascience* **10**, 1–4 (2021).
442 42. Shiraishi, H. & Tabuse, Y. The *Apl* I Restriction-Modification System in an Edible
443 Cyanobacterium, *Arthrospira* (*Spirulina*) *platensis* NIES-39, Recognizes the Nucleotide
444 Sequence 5′-CTGCAG-3′. *Biosci. Biotechnol. Biochem.* **77**, 782–788 (2013).
445 43. Roberts, R. J., Vincze, T., Posfai, J. & Macelis, D. REBASE-a database for DNA
446 restriction and modification: Enzymes, genes and genomes. *Nucleic Acids Res.* **43**, D298–
447 D299 (2015).
448
449

450

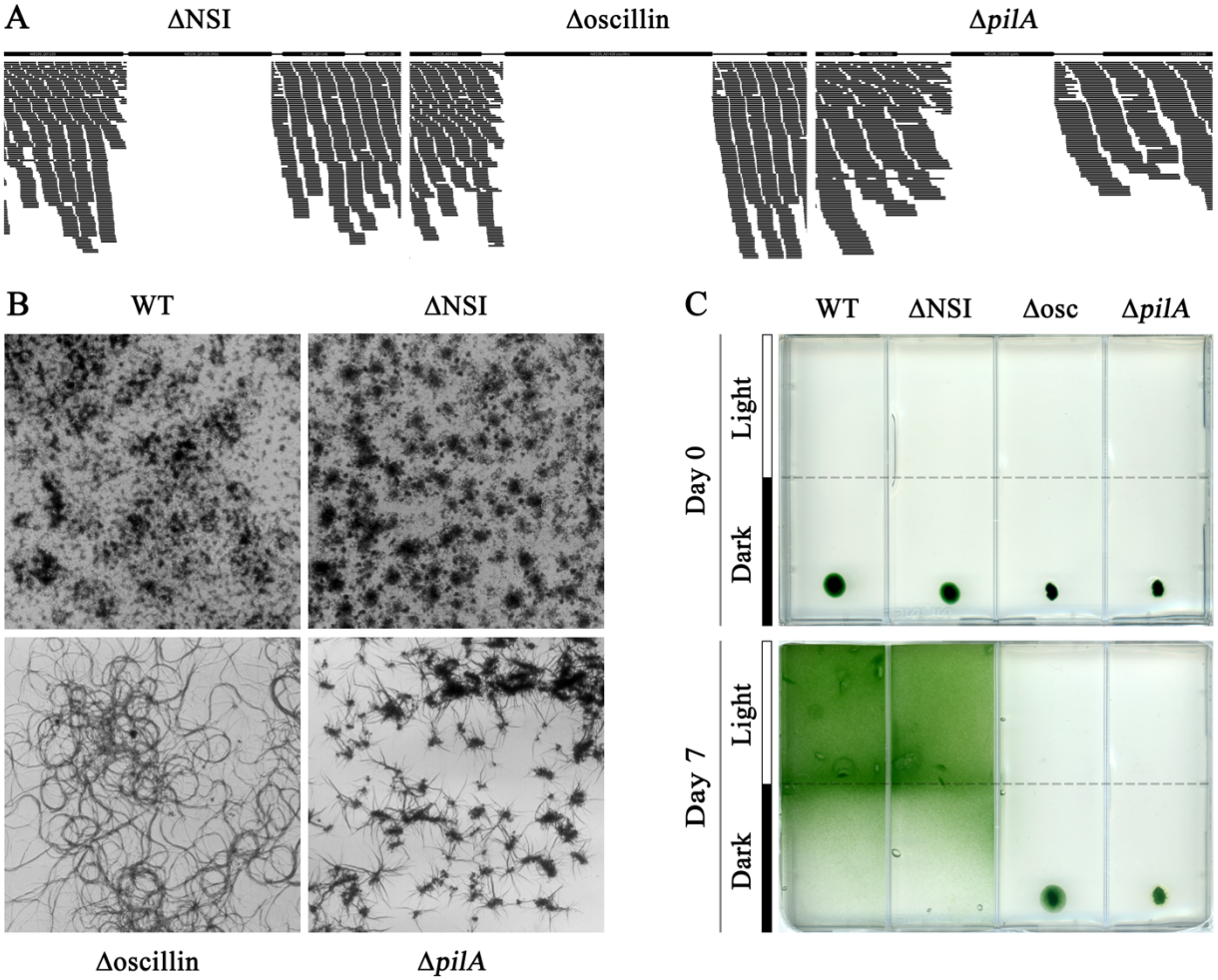

Figure 1. Confirmation and phenotyping of deletion mutants at three genomic loci. (**A**) Downsampled Illumina coverage for each genomic region that was swapped for *aadA.co*. (**B**) Images showing colony morphology on agar plates for the WT and each deletion strain. (**C**) Images depicting colony position on agar plates at Day 0 (top) and Day 7 (bottom) for the WT and each deletion strain. Strains were plated in the dark, and light was available to the upper half of the plate.

451

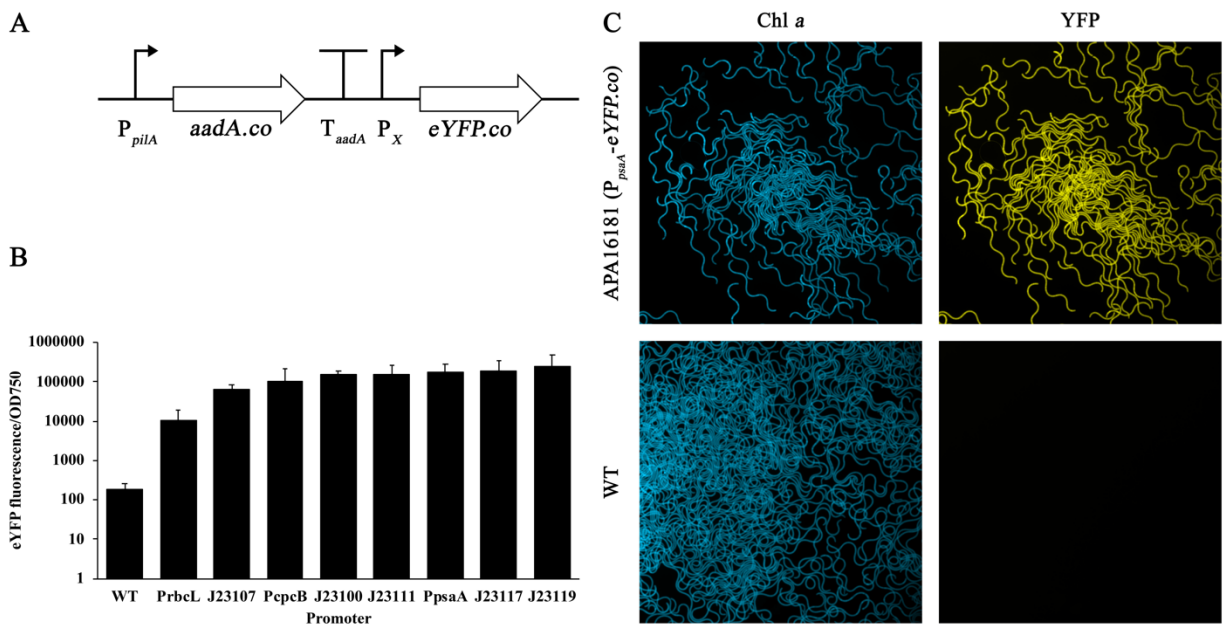

Figure 2. Fluorescent reporter and promoter characterization. (**A**) Schematic of the mutant genotypes for *eYFP.co* expression at the *pilA* locus: P_{pilA} drives expression of *aadA.co*, which is terminated by T_{aadA}. Downstream, one of three native promoters drives expression of the *eYFP.co* gene. (**B**) Relative promoter strength for three native *A. platensis* promoters and the five J23-series promoters. Error bars represent standard deviations of technical replicates. (**C**) Fluorescence microscopy of the Δ*pilA*::*aadA.co*-P*psaA*-*eYFP.co* and WT strains showing Chl *a* autofluorescence of filaments under excitation at 587 nm, and YFP fluorescence under excitation at 485 nm.

452

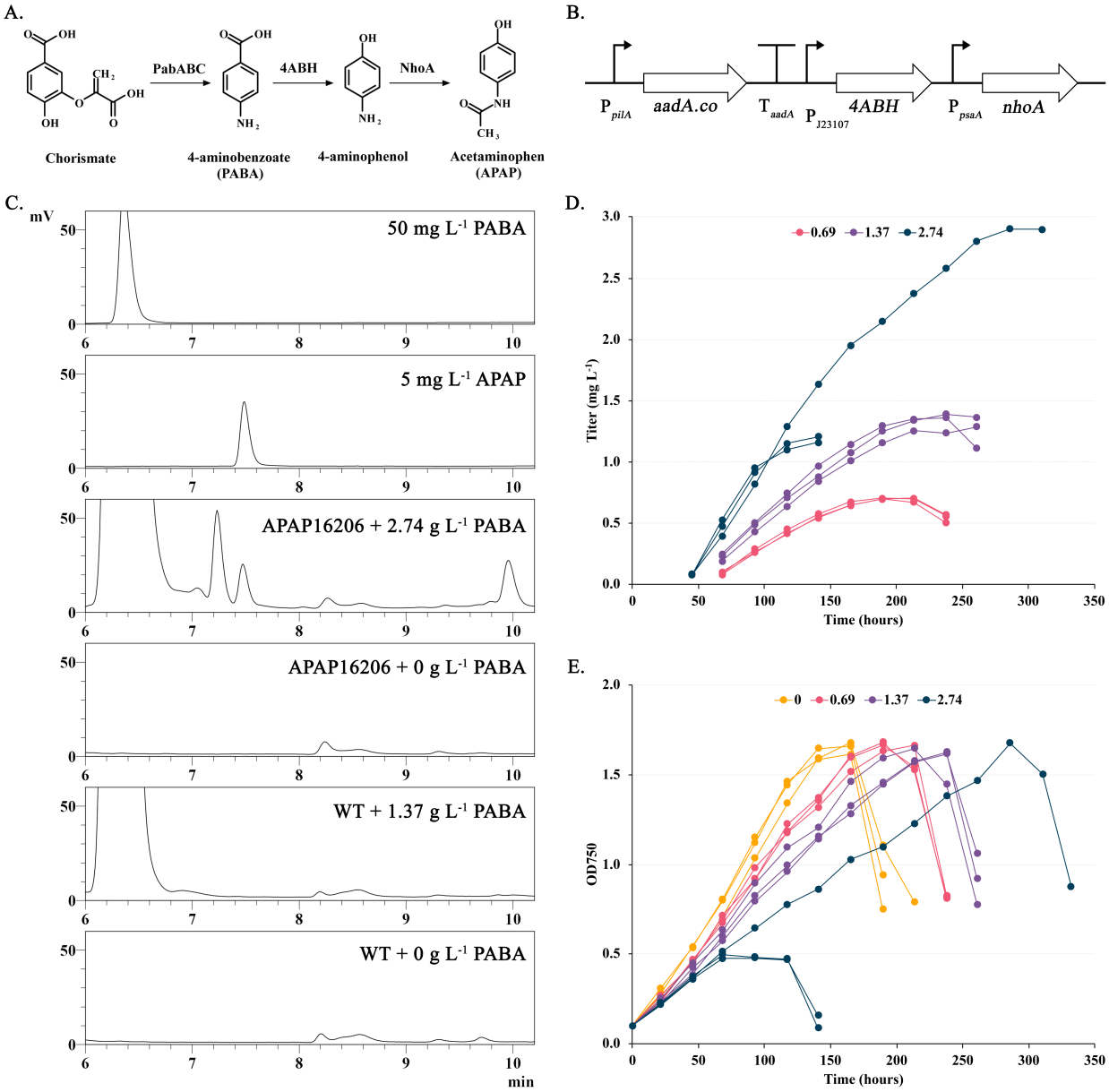

Figure 3. Figure 3. Acetaminophen (APAP) production in *A. platensis* APA16206. (A) The pathway for APAP production from para-aminobenzoic acid (PABA) uses the enzyme 4ABH to convert PABA to 4-aminophenol, which is then converted to APAP by NhoA. (B) Schematic for the APAP production pathway at the *pilA* locus in APA16206. (C) HPLC chromatograms showing peaks eluting between 6 and10.2 min for PABA and APAP standards along with APA16206 and WT strains with and without PABA supplementation. (D) APAP titer over time in APA16206 when supplemented with 0.69, 1.37, and 2.74 g L^{-1} PABA. (E) Growth of APA16206 with and without PABA supplementation at 0, 0.69, 1.37, and 2.74 g L^{-1}.